Torsional splitting of the intermolecular vibrations of phenol (H2O)1 and its deuterated isotopomers

M. Schmitt, Ch. Jacoby, and K. Kleinermanns

Citation: J. Chem. Phys. **108**, 4486 (1998); doi: 10.1063/1.475860
View online: http://dx.doi.org/10.1063/1.475860
View Table of Contents: http://jcp.aip.org/resource/1/JCPSA6/v108/i11
Published by the American Institute of Physics.

Torsional splitting of the intermolecular vibrations of phenol $(H_2O)_1$ and its deuterated isotopomers

M. Schmitt, Ch. Jacoby, and K. Kleinermanns
Heinrich-Heine-Universität Düsseldorf, Institut für Physikalische Chemie und Elektrochemie I, D-40225 Düsseldorf, Germany

(Received 11 February 1997; accepted 10 December 1997)

The intermolecular vibrations of phenol–water and their tunneling (torsional) splittings have been assigned in the S_1 state by mass resolved spectral hole burning. The abundance of transitions in the low frequency region of the spectra can be traced back to torsional tunneling of the water moiety, which splits all vibronic levels. Especially the in plane wag vibration β_2 exhibits a large splitting which points to a strong coupling with the H_2O torsion τ and a substantial lowering of the effective torsional barrier after β_2 excitation. Based on the discrimination of different isotopomers and their isomers and of the torsional sublevels a reassignment of some intermolecular transitions could be given. © *1998 American Institute of Physics.* [S0021-9606(98)01211-2]

I. INTRODUCTION

In recent years phenol–water clusters received considerable attention as model system for hydrogen bonding and solvent–aromatic solute interactions. Structure, dynamics and intermolecular vibrations of phenol$(H_2O)_1$ have been subject to a plethora of publications[1–31] due to its relatively small size, which allows theoretical predictions on an adequate level of theory, and easy experimental accessibility because of its abundant formation in a molecular beam and little fragmentation after ionization. The development of new laser spectroscopical methods and the application of computational methods on high levels of theory led to a rather profound knowledge about this cluster. Nevertheless its intermolecular vibrations are not fully assigned yet.

This paper belongs to a series of publications on hydrogen bonded phenol–water clusters based on high resolution spectroscopy and double resonance techniques. The first paper was mainly concerned with the geometric structure of phenol$(H_2O)_1$ in the electronic ground state using microwave spectroscopy for analysis.[1] The second paper extends the examination to the structure and to H_2O torsional tunneling in the electronically excited state based on rotationally resolved UV (ultraviolet)-spectroscopy.[2] The analysis of the rotational constants yielded a cluster structure with a nearly linear -OH$\cdots$O hydrogen bond and a *trans*-position of the water protons with respect to the aromatic ring. The plane containing phenol bisects the plane of the water molecule leading to a *trans*linear structure with C_s-symmetry.

The aim of this study[3] is a further inquiry of the torsional motion of the water moiety and its effect on the intermolecular vibrations of phenol$(H_2O)_1$ with spectral hole burning. This UV–UV double resonance technique is able to distinguish between vibrational transitions originating from different ground state levels.[4] The technique of SHB (spectral hole burning) employed in this investigation has already been applied to molecular beam studies of other hydrogen bonded hydroxyaromatic clusters.[5,6] Due to the internal rotation of the water moiety which interchanges the hydrogen atoms of the water molecule, there are two ground state tunneling levels. The eigenfunction of the $\sigma=0$ state is gerade $(+)$ with respect to reflection at the tunneling barrier while the $\sigma=1$ eigenfunction is ungerade $(-)$. The electronic origin band of phenol$(H_2O)_1$ therefore consists of two torsional components 0^+-0^+ and 0^--0^- according to the $+\leftrightarrow+$ and $-\leftrightarrow-$ selection rules (see Appendix). We show that all vibrational transitions are split into two components, which we label according to the symmetries of these subtorsional levels. The size of the splitting is a measure for the change of the effective torsional barrier after excitation of the respective vibration.

The 1:1 cluster has six intermolecular normal modes which arise from the loss of three rotations and three translations after complexation. These vibrations are the out of plane and in plane bend vibrations ρ_1 and β_1, the torsion and intermolecular stretch vibration τ and σ and the out of plane and in plane wag vibrations ρ_2 and β_2, respectively. The torsion and the wag vibrations show large displacements localized mainly on the H atoms of the H_2O molecule. Thus large anharmonicities and considerable isotopic shifts due to deuteration can be expected for these vibrations. The in plane wagging motion would lead to a *cis*-linear configuration which represents no minimum on the potential energy surface but appears as smaller gradient near the β_2 $(v=1)$-energy. Its harmonic frequency is therefore considerably reduced in an anharmonic calculation[7] (from 224 cm^{-1} to 147 cm^{-1}). A 180° torsion about the hydrogen bond would bring the *cis*-form back to the *trans*-linear configuration. This indicates that the torsional motion of the water moiety about the hydrogen bond axis is strongly coupled to the β_2 vibration. Two-dimensional *ab initio* calculations indeed demonstrate this effect.[7]

We show in the following, that particularly the β_2 vibration exhibits a large torsional splitting in the electronic ground and excited state which points to a substantial β_2-τ coupling as expected from theory.

A rotational analysis of the internal vibrations and their

tunneling splittings by Helm, Vogel and Neusser follows this publication.[8]

II. EXPERIMENT

The resonant two photon ionization (R2PI) measurements were carried out using the frequency doubled output of a Nd:YAG (Spectra Physics, GCR170) pumped dye laser (LAS, LDL205) operated with Fluorescein 27. For spectral hole burning another Nd:YAG (Spectra Physics GCR3) pumped dye laser (LAS, LDL205) with second harmonic generation (SHG) counterpropagates the first laser in the ionization region. The fundamental of the hole burning laser was used together with its second harmonic to improve the hole burning signal.

The apparatus used for spectral hole burning and for R2PI consists of a source chamber pumped with a 1000 l/s oil diffusion pump (Alcatel) in which the molecular beam is formed by expanding a mixture of helium, phenol and water through the 300 μm orifice of a pulsed nozzle (General Valve, Iota One). The skimmed molecular beam (Beam Dynamics Skimmer, 1mm orifice) crosses the laser beam(s) at right angles in the ionization chamber. The ions are extracted in a modified Wiley–McLaren type time-of-flight (TOF) spectrometer perpendicular to the molecular and laser beams and enter the third (drift)chamber, where they are detected using multi channel plates (Galileo). Typical mass resolution of the spectrometer is $m/\Delta m = 500$. Ionization and drift chamber are pumped with a 150 l/s rotatory pump (Leybold), respectively. The vacuum in the three chambers was $1 \cdot 10^{-3}$ mbar (source), $5 \cdot 10^{-5}$ mbar (ionization) and $1 \cdot 10^{-7}$ mbar (drift region), respectively, with beam on. The gridless linear TOF (Bergmann Meβgeräte Entwicklung) has some special features which will be described in the following.

Not all the ions, which are extracted from the ionization chamber, are produced by ionizing molecules of the supersonic jet. The laser ionizes residual gas molecules as well, which cause a strong but time-independent background signal. These background ions are strongly suppressed by applying a linear voltage ramp to the acceleration plates. Both the starting time and the slope of the voltage ramp are chosen so that only ions which travel with the velocity of the molecular beam are focused to the detector whereas background ions are destroyed at the walls. Furthermore the range of cluster sizes which are transmitted through the spectrometer can be varied by these parameters. A small aperture between ionization chamber and drift chamber increases the rejection of unwanted ions.

The optimization of the field geometry led to a comparably large detection volume (50 mm^3) in the ionization chamber without loss of resolution, due to potential energy uncertainty. Furthermore the sensitivity of the detection is increased by postacceleration of the signal ions in a Daley like converter. This increase in kinetic energy greatly enhances the yield of secondary electrons in the MCP (microchannel plate).

Ions, produced by the intense hole burning laser, perturb the experiment in a twofold manner: They distort the electric acceleration field and saturate the MCP detector thus decreasing the sensitivity for detection of the signal ions. To remove the undesired hole burning ions, the voltage of the repeller plate is first set to a negative potential. Shortly before the analyzing laser crosses the molecular beam the field is reversed for 10 μs using a fast push–pull high voltage switch (Behlke, GHTS60). For an optimal separation of hole burning and signal ions the lasers were delayed by 400–600 ns.

The resulting TOF signal was digitized by a 500 MHz digitizing oscilloscope (TDS 520A, Tektronix) and transferred to a computer, where the TOF spectrum was recorded by means of a program written in LABVIEW (National instruments). This program allowed us to record as many mass traces as necessary, to control the scanning of the laser and to display, save and plot the spectrum.

The Q-switch of the laser(s), the TOF voltage ramp and the HV-switch were triggered by a digital delay generator (Stanford DG535) together with a homebuilt delay generator for the triggering of laser flashlamps and pulsed nozzle. Timing stability was better than 2 ns.

The phenol–water clusters have been deuterated by coexpanding an appropriate mixture of H_2O and D_2O, kept at -5 °C together with phenol (Merck, p.A.) at room temperature in 1 to 2 bar of Helium. Within a few hours the partially and completely deuterated clusters were in a sufficient stable equilibrium, which allowed us to take the hole burning spectra of each species. The deuteration takes place at the phenolic H-atom or at the water molecule. Deuteration of the aromatic ring could be excluded under these conditions via NMR (nuclear magnetic resonance) spectroscopy. In the following ''totally deuterated'' refers to the three exchangeable H atoms (d_3).

III. SELECTION OF STATES

We utilized the technique of spectral hole burning to obtain a selection of states. A (hole burning) laser, which is tuned over the region of interest, induces a population transfer while, a few hundred nanoseconds later, the mass resolved photoionization signal of a resonantly excited transition acts as probe of this population. Every time the transitions induced by probe laser and hole burning laser share a common ground state level, the population of the ground state is reduced, what is detected as a decrease in probe signal.

In order to assign intermolecular vibrations of the phenol-water cluster, spectra of the different deuterated isotopomers of this cluster were taken. While only one isotopomer exists for the undeuterated (h_3) and the totally deuterated (d_3) cluster, there are two distinct isomers of the d_1 and d_2 clusters, respectively. These isomers cannot be distinguished by conventional mass resolved R2PI. Beyond this, an additional complication of the vibronic spectra is imposed by the existence of states of different torsional symmetry. From high resolution LIF (laser induced fluorescence) spectroscopy it is known, that the electronic origin of phenol $(H_2O)_1$ is split by 0.85 cm^{-1} into two torsional components.[8] We use UV–UV double resonance spectroscopy for the separation of different isomers and for distinction of states of different torsional symmetry.

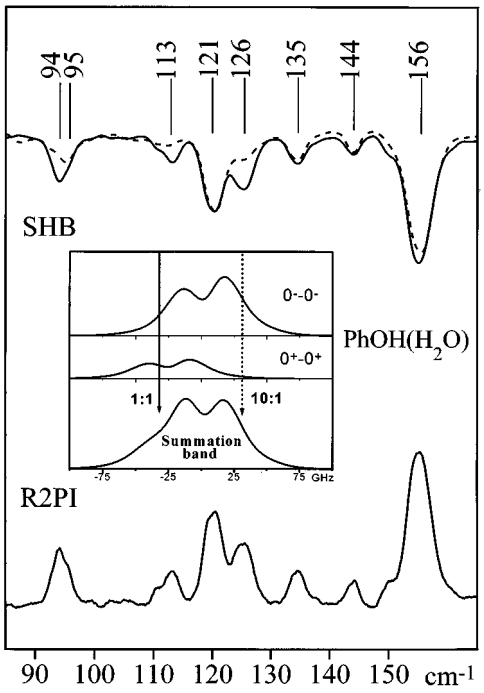

FIG. 1. R2PI (lower trace) and hole burning spectra (upper trace) of $PhOH(H_2O)$ when analyzing the low frequency side at 35 994 cm^{-1} (continuous line) and the high frequency side at 35 998 cm^{-1} (dashed line) of the electronic origin. The absolute frequencies of all SHB and R2PI spectra have been calibrated by recording the iodine absorption spectrum and comparison to tabulated iodine absorption frequencies. Absolute frequency accuracy is better than 0.5 cm^{-1}. The inset shows a simulation of the electronic origin band of phenol(H_2O), separated into its subtorsional components. The arrows mark the energy for low frequency and high frequency excitation, respectively. The rotational constants, torsional splitting and temperature for the simulation have been taken from Ref. 2.

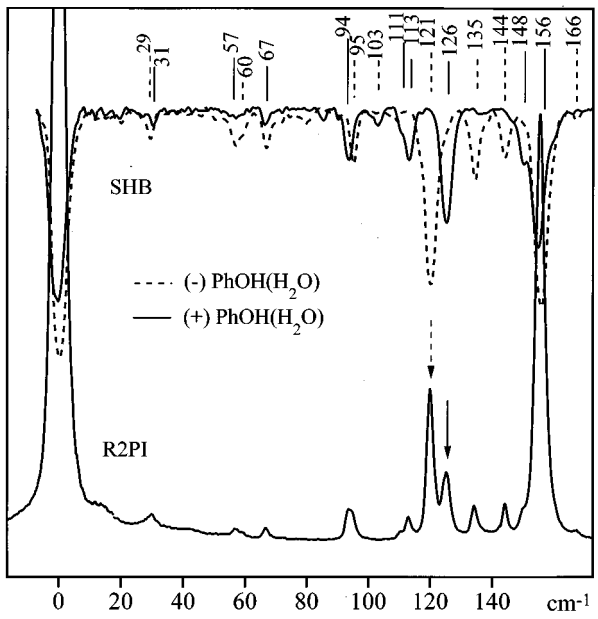

FIG. 2. R2PI (lower trace) and hole burning spectra (upper trace) of $PhOH(H_2O)$ between the electronic origin and the stretch vibration when analyzing the band at 121 cm^{-1} (dashed line) and at 126 cm^{-1} (solid line). The relative frequencies refer to the corresponding torsional component of the electronic origin. The values of the relative frequencies are marked by dotted lines if they belong to the $(-)$ component and by solid lines if they belong to $(+)$ or both components. This notation remains for all following figures.

Of course the first task is to find a band of pure symmetry. There are different ways to achieve this, depending on the size of the torsional splitting. If the torsional splitting is large compared to the width of the vibronic bands, state labeling will be no problem. Unfortunately in the case of the phenol-water cluster the torsional splitting of the electronic origin is of the magnitude of the linewidth or even smaller. Therefore the wings of the origin are analyzed (inset in Fig. 1) and pure symmetry species are identified by observing the intensity changes in the spectra, cf. Fig. 1. Once a band of pure symmetry is found, it can be utilized for improved analysis, e.g., the band at 126 cm^{-1} in Fig. 1. This method was applied to take the SHB spectra of the undeuterated phenol$(H_2O)_1$ cluster (Sec. IV A).

The isomers of the d_1 and d_2 clusters were discriminated via the intermolecular stretch vibrations of phenol(H_2O), phenol(HDO) and phenol(D_2O), cf. Figs. 3 and 5. The assignment of the intense stretch vibrations in these clusters is straightforward, due to the accurately predictable isotopic shifts. Their frequencies are sufficiently different to be useful for SHB analysis. Transitions of pure torsional symmetry in the d_1 isomers are identified by comparison to the h_3 spectrum, see the R2PI spectra in Figs. 2 and 3. The assignment for the d_2 isomer PhOD(HDO) was achieved by comparison to the PhOH(HDO) spectrum, see Figs. 3 and 5.

If the splitting becomes too small or more than two bands overlap, one has to step the analysis laser over the region of interest and take a hole burning spectrum at each position. This method was chosen for the investigation of the

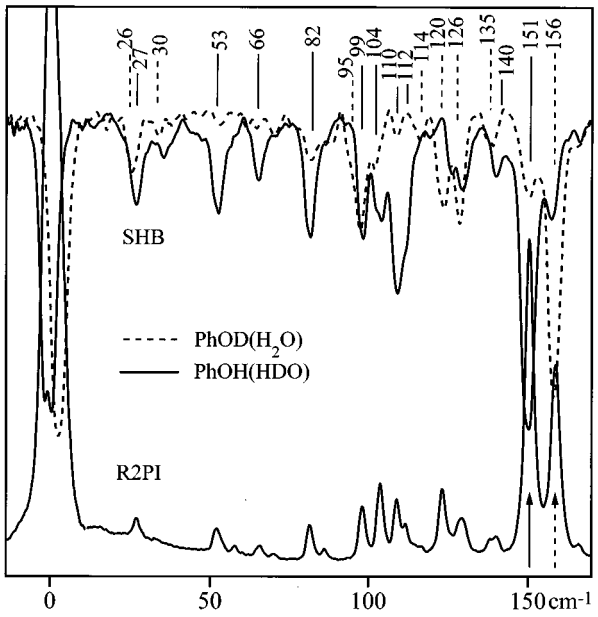

FIG. 3. R2PI (lower trace) and SHB spectra of the d_1 isotopomers of the phenol-water cluster in the region of the electronic origin. The analyzed bands are the stretch vibrations at 151 [PhOH(HDO), solid line] and 156 cm^{-1} [PhOD(H_2O), dashed line], respectively. The relative frequencies refer to the electronic origin of the corresponding isotopomer.

TABLE I. Absolute frequencies of the different deuterated isotopomers of the phenol-water cluster and their torsional splittings.

Isotopomer	Electronic origin [cm^{-1}]	Torsional splitting [cm^{-1}]
PhOH(H_2O)	35 996.3	0.85[a]
PhOD(H_2O)	36 000.6	0.7
PhOH(HDO)	35 997.5	0.4
PhOD(HDO)	36 001.1	0.2
PhOH(D_2O)	35 998.7	<0.1
PhOD(D_2O)	36 003.5	<0.1

[a]Exact value from Lit (Ref. 2).

d_3 isotopomer, which has a small torsional splitting in both electronic states, due to its large reduced mass (Sec. IV D).

In the case of phenol$(H_2O)_1$ and *d*-phenol$(D_2O)_1$ two different bands were found in the region of the electronic origin, while the origins of the d_1 and d_2 isotopomers are comprised of four bands (two different isomers and two different torsional symmetries). Upon each of these bands a complete vibrational ladder is built. All experimental frequencies given in this paper refer to the absolute frequency of the corresponding vibrationless transition. Therefore most of our frequencies differ from former publications, in which the exact position of the electronic origin could not be determined due to the overlap of different isomers of one isotopomer. In the following we call both torsional components of the vibrationless electronic transition $0^+ \leftarrow 0^+$ and $0^- \leftarrow 0^-$ ''electronic origin''.

IV. EXPERIMENTAL RESULTS

A. R2PI and SHB of the h_3-cluster

The inset in Fig. 1 shows a convolution of the simulated electronic origin band of phenol$(H_2O)_1$ with our laser bandwidth (0.2 cm^{-1}). The spin statistical weight of 3:1 for the $(-)$ and $(+)$ bands was taken into account. The rotational constants and the torsional splitting used for the simulation are given in Ref. 2. The rotationally resolved spectrum of the origin is discussed in more detail in the following paper.[8]

From the relative intensities it is obvious, that excitation of the high frequency component of the electronic origin will lead to 10:1 preferential population of the $(-)$ torsional sublevel in the S_1 state, while pumping the low frequency side, both $(+)$ and $(-)$ components will be excited nearly equally.

Figure 1 shows the R2PI (lower trace) and hole burning spectra (upper traces) when analyzing the low frequency side at 35 994 cm^{-1} (solid line) and the high frequency side at 35 998 cm^{-1} (dashed line). The bands at 121, 135, 144, and 156 cm^{-1} hardly show any intensity difference. This situation is different for the bands at 94, 113, and 126 cm^{-1}. They vanish when exciting the high frequency side of the origin. According to the rotational analysis of the origin,[2] these bands are supposed to have $(+)$ character.

The band at 126 cm^{-1} was the strongest band which showed any effect in the hole burning spectrum and was therefore used for SHB analysis. Figure 2 shows the R2PI (lower trace) and hole burning spectrum when analyzing the

TABLE II. Intermolecular vibrational frequencies of all isotopomers of the phenol-water cluster in the S_1 state.

PhOH(H_2O)	PhOD(H_2O)	PhOH(HDO)	PhOD(HDO)	PhOH(D_2O)[a]	PhOD(D_2O)	Assignment
29.2 $(-)$	29.5 $(-)$	27.4 $(-)$	27.2 $(-)$	24.8[b]	25.0[b]	ρ_1^-
30.9 $(+)$	29.7 $(+)$	27.1 $(+)$	27.4 $(+)$			ρ_1^+
56.8 $(-)$		51.9 $(-)$	52.5 $(-)$	47.9	48.2 $(+)$	$2\rho_1^-$
57.2 $(+)$		53.0 $(+)$	54.1 $(+)$		48.3 $(-)$	$2\rho_1^+/\tau(1^+-0^+)$
					55.8 $(+)$	
59.5 $(-)$		58.1 $(-)$	58.5 $(-)$			$\tau(1^--0^-)$
67.1 $(+)$	67.1 $(+)$	65.4 $(+)$	66.4 $(+)$	59.3	59.9 $(+)$	β_1^+
66.7 $(-)$		66.2 $(-)$	66.7 $(-)$		60.0 $(-)$	β_1^-
		67.8 $(+)$				
94.3 $(+)$	94.9 $(+)$	81.9 $(+)$	83.3 $(+)$	77.9	78.6 $(+)$	$\tau(2^+-0^+)$
95.0 $(-)$	95.5 $(-)$	86.4 $(-)$	86.9 $(-)$			$\beta_1^- + \rho_1^-$
103.4 $(+)$						
111.2 $(+)$	111.6 $(+)$					$4\rho_1^+$
113.4 $(+)$	114.4 $(+)$	98.8 $(+)$	99.4 $(+)$	85.5	86.5 $(+)$	β_2^+?
120.5 $(-)$	120.3 $(-)$	104.0 $(-)$	104.5 $(-)$	87.6	88.5 $(-)$	β_2^-
		109.6 $(+)$	110.4 $(+)$			
125.9 $(+)$	126.2 $(+)$	112.2 $(+)$	113.3 $(+)$	103.1	103.5 $(+)$	β_2^+?
		130.1 $(+)$	132.0 $(+)$	120.3	120.6 $(+/-)$	$2\beta_1^+$
134.5 $(-)$	135.3$(-)$	130.7 $(-)$	131.5 $(-)$			$2\beta_1^-$
143.9 $(-)$	144.1$(-)$	139.5 $(-)$	141.6 $(-)$			X^-
148.4 $(+)$	148.0$(+)$	140.3 $(+)$		141.7	142.7 $(+)$	X^+
155.6 $(+)$	155.5 $(+)$	150.7 $(+)$	151.4 $(+)$	144.9	145.7 $(+)$	σ^+
155.6 $(-)$	155.8 $(-)$	150.7 $(-)$	151.3 $(-)$		145.1 $(-)$	σ^-
				150.3	150.9 $(+)$	$\tau(4^+\text{-}0^+)$
				154.1	154.6$(+)$	$\beta_1^+ + \beta_2^+$
					154.9 $(-)$	$\beta_1^- + \beta_2^-$
				158.0	158.7 $(+)$	$2\beta_2$?

[a]The symmetry species of this isotopomer could not be separated.
[b]Values taken from the R2PI spectra.

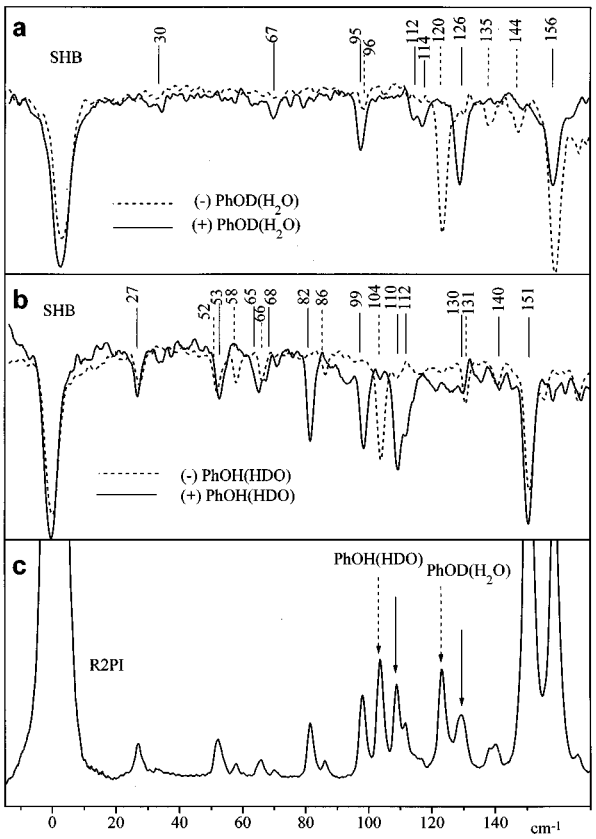

FIG. 4. SHB spectra of the PhOD(H_2O) cluster (a) and the PhOH(HDO) cluster (b) together with the R2PI spectrum (c). The analyzed bands for each isotopomer are marked with arrows in the R2PI spectrum. The (+) components are presented by solid lines, (−) components by dashed lines. All relative frequencies refer to the torsional component of the corresponding electronic origin.

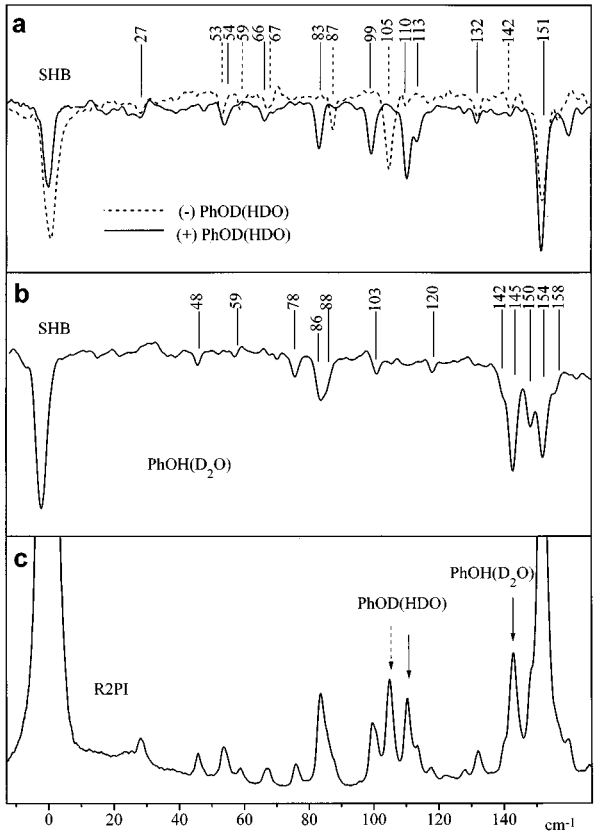

FIG. 5. R2PI (c) and SHB spectra of the PhOD(HDO) cluster (a) and the PhOH(D_2O) cluster (b). The analyzed bands are marked with arrows in the R2PI spectrum. The (+) components are presented by solid lines, (−) components by dashed lines.

band at 126 cm^{-1}(upper trace, continuous line). Obviously the band at 121 cm^{-1} vanishes completely in the hole burning spectrum upon analysis of the 126 cm^{-1} (+) band and must therefore belong to the (−) subtorsional component. Pumping the 121 cm^{-1} band and scanning the hole burning laser over the same region leads to the second hole burning spectrum given in Fig. 2 (upper trace, dashed line). An assignment of each line of the R2PI spectrum to the symmetry of the torsional sublevel is now possible.

The bands at 29/31, 57, 67, 94/95, and 156 cm^{-1} comprise two components of different torsional symmetry. The bands at 103, 111, 113, 126, and 148 cm^{-1} have pure (+) character, while the bands at 60, 121, 135, 144, and 166 cm^{-1} belong to the (−) torsional subgroup. The stretch vibration at 156 cm^{-1} shows a similar (small) torsional splitting as the electronic origin (0.9 cm^{-1}, cf. Table I). The corresponding bands can be described as $\sigma^+ \leftarrow 0^+$ and $\sigma^- \leftarrow 0^-$ transitions. The experimental frequency shifts relative to their (+) or (−) electronic origin and the assignments to the torsional symmetries are presented in Table II.

B. R2PI and SHB of the d_1-cluster isomers

The d_1-isotopomers of the phenol(H_2O)$_1$ cluster have been produced by coexpanding a 1:1 mixture of D_2O and H_2O, acidified with citric acid, together with phenol in 1 bar He. The recorded mass trace of the d_1-isotopomers of phenol(H_2O) at $m/e=113$ contains transitions from both possible isomers: PhOD(H_2O) and PhOH(HDO). The easiest way to distinguish between these isomers is to excite the stretch vibrations of both clusters, which are clearly separated due to the different reduced masses.

Figure 3 shows the hole burning spectra of the d_1-isomers taken upon excitation of both stretch vibrations (upper traces) together with the corresponding R2PI spectrum (lower trace). The dashed line of the SHB spectra represents the PhOD(H_2O) cluster, the solid line the PhOH(HDO) cluster. One has to bear in mind that the experimental (relative) frequencies refer to different electronic origins. The origin bands of both tautomers are distinctly separate giving transition energies of 35 997.5 cm^{-1} and 36 000.6 cm^{-1}, respectively. These values differ slightly from the values presented by Dopfer *et al.*[31] because they determined the frequencies from a deconvolution of the origins, which could not be distinguished by R2PI. The absolute frequencies of the electronic origins of all isotopomers are presented in Table I.

After separation of the bands according to their isomeric descent the symmetry species had to be distinguished. We started with investigations of the PhOD(H_2O) spectrum because of its similarity to the PhOH(H_2O) spectrum. Pure (+) and (−) bands in the h_3 cluster were located at 121 cm^{-1} (−) and 126 cm^{-1} (+) and guided us in the choice of suit-

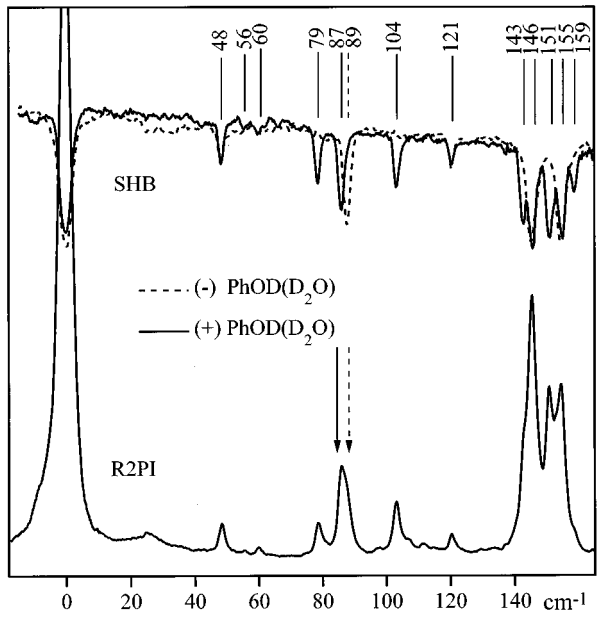

FIG. 6. SHB and R2PI spectra of the PhOD(D_2O) cluster. The analyzed positions are marked with arrows in the R2PI spectrum. (+) components are presented by solid lines, (−) components by dashed lines.

able analysis frequencies for the d_1-cluster. The SHB spectra of the PhOD(H_2O) cluster are presented in Fig. 4(a). The separation of the (+) and (−) component of the electronic origin is determined to be 0.7 cm^{-1}. The bands at 30, 67, 95, 112, 114, 126, and 156 cm^{-1} belong to the (+) component of the torsion, the bands at 30, 96, 120, 135, 144, and 156 cm^{-1} to the (−) component.

The vibrational pattern at 104/110 cm^{-1} in the R2PI spectrum of the d_1-clusters looks similar to the 120/126 pattern in the PhOD(H_2O) and PhOH(H_2O) spectra. Figure 3 shows, that this pair belongs to the PhOH(HDO) cluster. Transitions of pure symmetry can be obtained by using these bands for SHB analysis [Fig. 4(b)]. The torsional splitting of the electronic origin of this cluster could be determined to be 0.4 cm^{-1}, cf. Table I. The stretch vibration at 151 cm^{-1} as well as three vibrations at 27, 52/53, 65/66, 130/131, and 140 cm^{-1} comprise both torsional symmetries. Pure (+) bands are found at 68, 82, 99, 110, and 112 cm^{-1}, pure (−) bands at 58, 86, and 104 cm^{-1}. The larger number of transitions in the PhOH(HDO) cluster compared to PhOH(H_2O) and PhOD(H_2O) is due to the lowered symmetry ($C_s \rightarrow C_1$) in this cluster.

The vibrational frequencies together with the symmetry assignments of both isotopomers are summarized in Table II.

C. R2PI and SHB of the d_2-cluster isomers

The d_2-isotopomers of the phenol-water cluster have been produced by coexpanding a 2:1 mixture of D_2O and H_2O, acidified with citric acid, together with phenol in 1 bar He. As in the case of the d_1-cluster, four different electronic origins with separate vibrational ladders should be distinguishable.

The first step is the separation of transitions from different isomers of the d_2-cluster. While analysis of the band at 145 cm^{-1} in Fig. 5(c) resulted in a spectrum of the pure PhOH(D_2O) shown in Fig. 5(b), the band at 151 cm^{-1} proved to be an overlapping band of both isotopomers. Therefore the SHB spectrum analyzed through this band was merely a mirror image of the R2PI spectrum. Either the PhOH(D_2O) bands were overlapped by PhOD(HOD) bands, or the torsional splittings were too small to allow the separation of the torsional symmetries in Fig. 5(b). The region of the stretch vibration between 140 and 160 cm^{-1} in Fig. 5(b) consists of more bands than visible in the H_2O and HDO spectra but is strikingly similar to the PhOD(D_2O) spectrum and will be discussed later.

Guided by the similarity of the PhOD(HDO) and the PhOH(HDO) spectrum, the bands at 105 and 110 cm^{-1} are chosen for analysis of PhOD(HDO), cf. Fig. 5(c). Figure 5(a) shows the (+) bands of PhOD(HDO) at 27, 54, 66, 83, 99, 110, 113, 132, and 151 cm^{-1}, while the (−) bands are observed at 27, 53, 59, 67, 87, 105, 132, 142, and 151 cm^{-1}. The torsional splitting of the origin is determined to be 0.2 cm^{-1} which is close to our laser bandwidth. The sequence of origin bands in Fig. 5(a) supports our (+) and (−) assignments.

The absolute frequencies of the electronic origins could be located at 36 001.1 cm^{-1} for the PhOD(HDO) cluster and at 35 998.7 cm^1 for the PhOH(D_2O) cluster, cf. Table I. The vibrational frequencies relative to the electronic origin of each isomer and the symmetry assignments of PhOD(HDO) are summarized in Table II.

D. R2PI and SHB of the d_3-cluster

As in the case of the PhOH(D_2O) cluster the torsional splitting of the electronic origin of PhOD(D_2O) and of the stretch vibrations around 145 cm^{-1} was too small to be useful for SHB analysis. The transition at 87 cm^{-1} shows a shoulder in the R2PI spectrum and looks like the extension of the 113(+)/120(−) and 99(+)/105(−) sequence in the spectra of the clusters with H_2O and HDO, respectively. We stepped the analysis laser over this band and took a hole burning spectrum at each position. Figure 6 shows the SHB spectra obtained by analysis of the low and high frequency part of this band, respectively. Nearly complete separation of the torsional components was achieved. The symmetry assignments are summarized in Table II.

Pure (+) components were found at 56, 79, 87, 104, 143, 151, and 159 cm^{-1}, while a pure (−) component was only observed at 89 cm^{-1}. The bands at 48, 60, 121, 146, and 155 cm^{-1} comprise both symmetries. The R2PI spectrum in the region of the stretch vibration at the mass of the d_3 isotopomer appears to be totally different from all other spectra and consists of at least five bands. The similarity of the PhOD(D_2O) and PhOH(D_2O) spectra in Figs. 5(b) and 6 in this region becomes only obvious after separation from the dominating PhOD(HDO) stretch vibration by spectral hole burning.

V. DISCUSSION

The intermolecular vibrational frequencies of all isotopomers of the phenol$(H_2O)_1$ cluster have been calculated for

TABLE III. Intermolecular harmonic vibrational frequencies (cm^{-1}) of all phenol–water isotopomers, calculated by a normal mode analysis based on a 6-31 G(d,p) optimized geometry. The values in brackets give the percentage deviations from the h_3 isotopomer.

	ρ_1	β_1	τ	σ	ρ_2	β_2
PhOH(H_2O)	33.6	58.8	103.3	154.8	214.7	223.9
PhOD(H_2O)	33.4 (−0.6)	58.5 (−0.5)	103.3 (±0)	154.3 (−0.3)	203.8 (−5.1)	223.7 (−0.1)
PhOH(HDO)	32.2 (−4.2)	56.6 (−3.7)	87.8 (−15.0)	146.6 (−5.3)	179.8 (−16.3)	213.8 (−4.5)
PhOD(HDO)	32.0 (−4.8)	56.3 (−4.3)	87.8 (−15.0)	146.0 (−5.7)	175.9 (−18.1)	210.7 (−5.9)
PhOH(D_2O)	31.1 (−7.4)	55.3 (−6.0)	76.8 (−25.7)	142.0 (−8.3)	163.8 (−23.7)	182.8 (−18.4)
PhOD(D_2O)	30.9 (−8.0)	54.9 (−6.6)	76.8 (−25.7)	141.6 (−8.5)	159.8 (−25.6)	182.7 (−18.4)

comparison with the experimental frequencies shown in Table II. The geometry has been tightly optimized at the Hartree–Fock SCF (self-consistent field) level with the 6-31G(d,p) basis set, using the GAUSSIAN 94 program package.[32] The normal mode analysis was performed by using the analytical second derivatives of the potentials. Table III presents the harmonic vibrational frequencies of all isotopomers together with the frequency differences to the h_3 isotopomer. The mode assignment discussed in the following is based on these results and the anharmonic calculations of Schütz *et al.*[7]

Table II shows that the torsional splittings of the vibronic transitions are in many cases different from the splitting of the electronic origin. The splitting of the vibrational bands almost always exceeds the torsional splitting of the origin. For some of them, e.g. the in plane wag vibration β_2, the splitting is especially large suggesting a strong coupling to the torsion. For other vibrations like the stretch vibration in the S_1 state, there is virtually no difference to the splitting of the electronic origin.

A. The bend vibrations ρ_1 and β_1

The lowest frequency band in the R2PI spectra of phenol$(H_2O)_1$ is located at 30 cm^{-1}. The corresponding transition in the PhOH(HDO) and in the PhOD(HDO) isotopomer lies at 27 cm^{-1}. The frequency of this vibration in the d_3-isotopomer at 25 cm^{-1} is taken from the R2PI spectrum, because it did not show up in the SHB spectrum due to unfavorable signal to noise ratio. The frequency, as well as the calculated small isotopic shift (Table III) of this transition, implies an assignment to the out of plane bend vibration ρ_1. This vibration is nontotally symmetric for C_s species like the h_3 and d_3-clusters and therefore weak in spectra of these isotopomers. For PhOH(HDO) and PhOD(HDO) this symmetry is broken, and the vibration is substantially more intense, cf. the R2PI spectra in Figs. 4 and 5. In the h_3- and d_3-clusters with C_s symmetry the first overtone of this vibration should be allowed. The bands at 57 cm^{-1} in the h_3 spectrum and at 48 cm^{-1} in the d_3 spectrum are assigned to this overtone. In addition the ρ_1 overtone is also observed in the asymmetric (HDO) clusters, cf. Table II.

According to the *ab initio* calculations the first totally symmetric vibration is the in plane bend vibration β_1 which is calculated to lie at 59 cm^{-1} in the S_0 state of the h_3-isotopomer. The band at 67 $cm^{-1}$is close to that value. The experimental frequency decreases by 3% for the HDO clusters in fair agreement to the computations. The assignment of this band to the bend vibration β_1 is also confirmed by ZEKE (zero kinetic electron energy) measurements of the phenol-water cluster by Dopfer.[33] In the ZEKE spectrum, taken through the 67 cm^{-1} band, the most prominent progression in the ion is the combination of the stretch vibration with the in plane bend vibration. For the d-phenol(D_2O) cluster the frequency decreases to 60 cm^{-1} what appears to be too much compared to the computations. Nevertheless this band is assigned to the bend vibration because no other band comes into question.

B. The wag vibrations β_2 and ρ_2

The 121 cm^{-1} band has been assigned previously by different groups to the in plane wag vibration.[7,24,33] Our spectra clearly show, that the 121 cm^{-1} band is just a (−) torsional component. This is further supported by the rotational analysis given in the following paper.[8] In the vicinity there are two bands at 113 and 126 cm^{-1} with pure (+) character, which could be assigned to the (+) component of the in plane wag vibration. Dependent on the coupling between torsion and β_2 vibration, the sequence of the torsional components may be reversed compared to the electronic origin, allowing either of the two bands to be the (+) component of the 121 cm^{-1} (−) band, cf. Table II. The in plane wag vibration β_2 shows the largest torsional splitting of all intermolecular vibrations in the S_1 state, however, indicating a strong coupling between the β_2-mode and the torsion in agreement with theory.

The nontotally symmetric wag vibration ρ_2 of the h_3 isotopomer has a frequency of 214.7 cm^{-1} in the one-dimensional harmonic approximation. No evidence for the occurrence of this vibration could be found in the SHB spectra. The unassigned band X in Table II is a possible candidate if ρ_2 is substantially anharmonic. The band X shows little isotope shift, however, contrary to the harmonic calculations in Table III.

C. The torsional vibration τ

There are several bands in the symmetry labeled SHB spectra of each isotopomer which are of pure (+) or (−) torsional symmetry. Some of them cannot be explained by a torsional splitting of an intermolecular vibrational band solely. These bands may be due to pure torsional transitions from one of the torsional ground states 0^+ or 0^-. The interconversion path for the water hydrogen atoms must in principle be regarded to lie at least on a two-dimensional PES

TABLE IV. Transformation properties of the torsional angle α and the resulting representations of the free rotor and the high barrier limit, respectively.

	E	(12)	E^*	(12)*	Symmetry
α	α	$\alpha+\pi$	$-\alpha+\pi$	$-\alpha$	
$m=0$	1	1	1	1	A_1
m even	2	2	0	0	A_1+A_2
m odd	2	-2	0	0	B_1+B_2
v even	2	0	0	2	A_1+B_2
v odd	2	0	0	-2	A_2+B_1

resulting from the β_2/τ coupling. As a consequence the reduced internal rotation constant F is not conserved along this path. In our calculations we used an effective value of F which was obtained from the limiting case of a simple b axis rotation of the water moiety [$F(H_2O)=14.7$ cm^{-1}; $F(D_2O)=7.3$ cm^{-1}]. The energy levels and wave functions for the torsion have been calculated by solving the Schrödinger equation $H\Psi=E\Psi$ with an effective Hamiltonian of the form $H=-F(d^2/d\phi^2)+(1/2)\Sigma_n V_n\cdot(1-\cos n\phi)$ which is setup in the representation of the free rotor basis functions $\psi_m=(2\pi)^{-1/2}e^{im\phi}$ with $m=0,\pm1,\pm2\ldots$. The elements of the corresponding Hamiltonian matrix have been determined using the method described by Lewis *et al.*[34] The only potential term used in the series expansion of the Hamiltonian was the V_2 term. We performed several fits of the torsional barriers to the experimental transition frequencies of the h_3 and d_3 cluster using the Levenberg–Marquardt algorithm.[35] We had to saturate the hole burning step to overcome the problem of very small intensities of the torsional bands and could therefore perform no fit of the intensities.

The results of the best fits are discussed in the following. Barriers of 145 cm^{-1} for the S_0 and 110 cm^{-1} for the S_1-state nicely reproduce the torsional splitting of the origin (0.85 cm^{-1} obs./0.89 cm^{-1} calc.) and the $2^+\leftarrow0^+$ transition (94.3/94.3 cm^{-1}) in the h_3 isotopomer. The $2^-\leftarrow0^-$ transition is calculated to be at 152.9 cm^{-1} and should be more intense than the corresponding (+) transition, due to spin statistics. Unfortunately, any band at this frequency is hidden by the intense stretch vibration.

Using the same barriers and $F=B$ (D_2O) for the calculation of the torsional transitions of the d_3-cluster, the torsional splitting of the electronic origin ($<0.1/0.1$ cm^{-1}) as well as the $2^+\leftarrow0^+$ transition (78.6/77.3 cm^{-1}) and the $4^+\leftarrow0^+$ transition (150.9/149.7 cm^{-1}) are reproduced quite well. The $2^-\leftarrow0^-$ transition of this isotopomer, which should be located at 97 cm^{-1}, is however missing in the spectrum. Although this (−) transition should be weaker by a factor of 2 than the corresponding (+) component according to nuclear spin statistics of the fully deuterated isotopomer, the band should show up due to the good S/N ratio in the spectrum.

In the C_1-symmetric phenol(HDO) clusters, the $1^\pm\leftarrow0^\pm$ transitions become allowed. Using an F value of 10 cm^{-1}, the $1^-\leftarrow0^-$ transition is calculated to 58.5 cm^{-1}. The (−) bands at 58.1 cm^{-1} [PhOH(HDO)] and 58.5 cm^{-1} [PhOD(HDO)] can therefore be assigned to this torsional transition. The $1^+\leftarrow0^+$ transition is calculated to 50.1 cm^{-1}. In the SHB and R2PI spectra of PhOH(HDO) and PhOD(HDO) the $1^+\leftarrow0^+$ transition may be superimposed by the $2\rho^+\leftarrow0^+$ bands (see Table II).

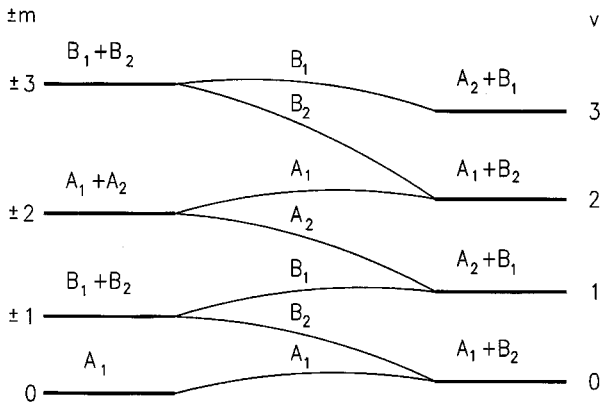

FIG. 7. Correlation diagram of the free rotor and harmonic oscillator limiting cases.

The 2^+-0^+ transition of phenol(HDO) is calculated to 83.2 cm^{-1} compared to experimental values of 81.9 cm^{-1} for PhOH(HDO) and 83.3 cm^{-1} for PhOD(HDO). The splitting of the origin is 0.3 cm^{-1} compared to experimental 0.4 cm^{-1} for PhOH(HDO) and 0.2 cm^{-1} for PhOD(HDO). Again the 2^--0^- transition expected at 116.7 cm^{-1} is missing.

The difficulties to assign the pure torsional transitions may arise from a negligible geometry change along the torsional coordinate upon electronic excitation. This leads to very weak torsional bands due to the Franck–Condon principle.

D. The stretch vibration σ

The stretch vibration is the most prominent feature in each spectrum of the different isotopomers beside the electronic origin. By analyzing the stretch vibrations in the mixed d_1- and d_2-isotopomers via ZEKE spectroscopy[31] it could clearly be shown, that the unusual intensity distributions in the stretch region of these spectra are due to different isotopomers and not to a Fermi resonance as concluded by Lipert and Colson.[24]

A quite unusual intensity pattern is observed in the region of the stretch vibration of the d-phenol(D_2O) cluster. The appearance of several bands is surprising, because for this cluster only one isotopomer can exist. Three of the bands at 143, 151, and 159 cm^{-1} are pure torsional (+) components, while the other at 146 and 155 cm^{-1} comprise both symmetries. A combination of the totally symmetric bend and wag vibrations β_1 and β_2 has the suitable symmetry and energy to constitute a Fermi dyade with the stretch vibration. Another possibility is a Fermi dyade comprised of the stretch vibration and the first overtone of the in plane wag vibration β_2. This assumption is based on a large negative anharmonicity for the β_2 vibration, contrary to the S_0 calculation in Ref. 7 with a positive anharmonicity for the β_2 vibration. The situation is even more complicated by a possible addi-

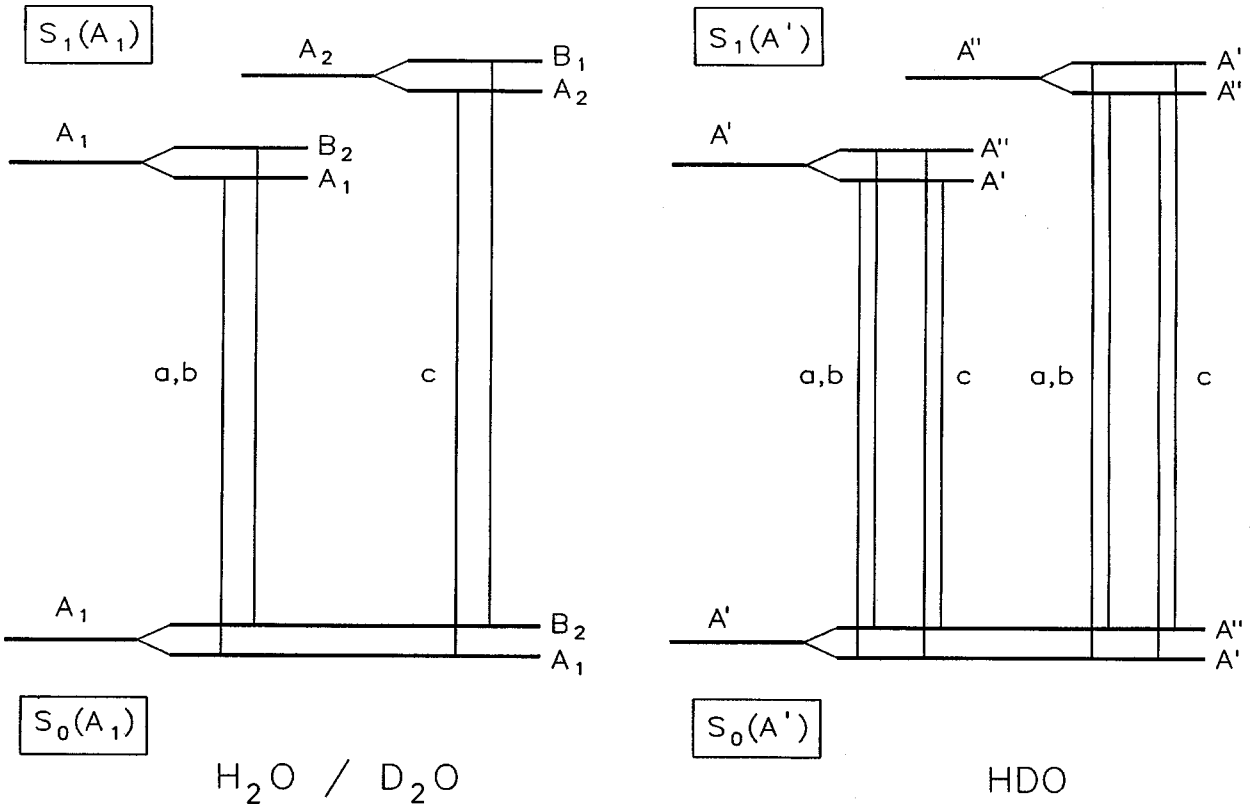

FIG. 8. Allowed vibronic transitions of $PhOH(H_2O)_1$ together with their polarizations.

tional interaction of the perturbed levels with pure torsional levels, which may show up in the quite intense pure (+) bands in this region. One of the bands, which may be responsible for this perturbation, is the 4^+-0^+ transition, which is calculated to be at 150 cm^{-1} as shown above.

VI. CONCLUSIONS

We could demonstrate that mass resolved UV–UV double resonance spectroscopy allows spectral discrimination of different isomers of one cluster isotopomer if at least the wings of two overlapping isomer bands are separated. Very detailed studies of vibrational and electronic spectral shifts in different isotope substituted species are feasible with this method and helpful to assign vibrations. Isomer selection of unsymmetrically substituted clusters like phenol-(HDO) is particularly interesting because it enables us to study symmetry forbidden optical transitions and large amplitude motions in slightly asymmetric multiple potentials. Tunneling due to flexible substituents in a molecule or cluster is quite common and may lead to very specific splittings and highly anharmonic progressions of vibrations with components along the tunneling coordinate. The method introduced in this paper allows an assignment of all optically accessible vibrational states according to their tunneling symmetry if the tunneling splitting is large enough for vibrational resolution. This may help to interpret vibronic spectra of fluxional molecules or clusters which show a seeming abundance of vibronic transitions.

This study contributes to a more detailed understanding of the in plane and out of plane bend and wag vibrations as well as the torsion and the intermolecular stretch mode of phenol(H_2O) and their coupling and tunnel splittings. The experimental data are basis for a fully six-dimensional quantum mechanical calculation of the coupled intermolecular vibrations of phenol(H_2O) which might be feasible in the future.

ACKNOWLEDGMENT

The authors gratefully acknowledge the financial support of the Deutsche Forschungsgemeinschaft (Schwerpunkt Molekulare Cluster).

APPENDIX: THE SYMMETRY OF THE PHENOL–WATER CLUSTER

The phenol-water cluster can be classified by the molecular symmetry group[36] G_4, which is isomorphic with the point group C_{2v}. The first element of this symmetry group is the identity E. The (12) operation can be described by a rotation around the b axis of the water moiety resulting in an equivalent conformer, in which the two hydrogen atoms are exchanged. The operation E^* is the inversion, i.e., the reflection of all spatial coordinates at the center of mass and $(12)^*$ is the product of (12) and E^*.

The torsional angle α is defined to be zero in the equilibrium geometry with the hydrogen atoms lying above and below the plane of symmetry. Application of the symmetry operations leads to the transformation properties of α given in the first row of Table IV. To obtain the symmetry species of the torsional levels, one has to correlate the levels of the free rotor limit and the high barrier limit. In the free rotor

model the wave functions are $|\pm m\rangle \equiv \psi_{\pm m} \propto e^{\pm im\alpha}$ ($m=0,1,2,\ldots$). Application of the symmetry operations R_i leads to the matrix representations

$$R_i\begin{pmatrix}|+m\rangle\\|-m\rangle\end{pmatrix}=\begin{pmatrix}a_{11} & a_{12}\\ a_{21} & a_{22}\end{pmatrix}\begin{pmatrix}|+m\rangle\\|-m\rangle\end{pmatrix},$$

with the characters $\chi_i = a_{11}+a_{22}$ given in Table IV. For $m=0$ there is only one function, which transforms like the totally symmetric representation A_1. For other values of m a consideration of the transformation properties of $|\pm m\rangle$ and therefore of α becomes necessary. For the identity operation E the character is obviously two. The character of (12) can be determined in the following way (the normalizing constant has been ignored):

$$\begin{aligned}(12)|\pm m\rangle &= e^{\pm im(\alpha+\pi)} = e^{\pm im\pi}e^{\pm im\alpha}\\ &= e^{\pm im\pi}|\pm m\rangle \Rightarrow \chi_{(12)} = e^{+im\pi}+e^{-im\pi}\\ &= 2\cos(m\pi) = 2(-1)^m.\end{aligned}$$

For the operations associated with spatial inversion the sense of rotation is reversed, so that all diagonal elements of the matrices are zero. The representations of the degenerate functions $|\pm m\rangle$ are summarized in Table IV. In the high barrier limit there are two harmonic potentials separated by an insurmountable barrier, so that the transformation properties of the vibrational states are given by the symmetry of the Hermitian polynomials $H_v(\alpha)$. Whereas the operations (12) and E^* lead to interconversion of the two equivalent conformers with $\alpha=0$ and $\alpha=\pi$, respectively, the character for the $(12)^*$ operation is $2(-1)^v$:

$$\begin{aligned}&(12)^*H_v(\alpha) = H_v(-\alpha) = (-1)^v H_v(\alpha),\\ &(12)^*H_v(\alpha+\pi) = H_v(-\alpha-\pi)\\ &\qquad = H_v(-\alpha+\pi) = (-1)^v H_v(\alpha+\pi).\end{aligned}$$

The representations of the harmonic wave functions are given in Table IV and a correlation of both limiting cases is shown in Fig. 7. The order of the torsional levels is $A_1, B_2, B_1, A_2, A_1, \ldots$.

The vibrational symmetries are A_1 for in-plane- and A_2 for out-of-plane-motions due to the symmetry species of the translational vectors along the molecular axes. These vectors transform like the components of the dipole moment. With both electronic states being totally symmetric the allowed transitions are displayed in Fig. 8. For phenol(H_2O/D_2O) we expect $+\leftrightarrow+$ and $-\leftrightarrow-$ selection rules. According to the analysis the ρ_1 fundamental transition is expected to have c-type rotational structure.

For the HDO-clusters there is no H-exchange anymore and the remaining elements are E and E^*. Application of E^* leads to an energetically equivalent conformer and therefore the $+/-$ designation which labels the linear combinations of the wave functions still holds. The transitions for the HDO-clusters, which has G_2 symmetry (isomorphic with the point group C_s), are also given in Fig. 8. The spin statistical weights of the two lowest levels are $1(A_1):3(B_2)$ for the H_2O-, $1(A'):1(A'')$ for the HDO- and $2(A_1):1(B_2)$ for the D_2O-clusters.

[1] M. Gerhards, M. Schmitt, K. Kleinermanns, and W. Stahl, J. Chem. Phys. **104**, 967 (1996).
[2] G. Berden, W. L. Meerts, M. Schmitt, and K. Kleinermanns, J. Chem. Phys. **104**, 972 (1996).
[3] This work is part of the dissertation of Ch. Jacoby.
[4] R. J. Lipert and S. D. Colson, J. Phys. Chem. **93**, 3894 (1989).
[5] R. J. Lipert and S. D. Colson, Chem. Phys. Lett. **161**, 303 (1989).
[6] (a) M. Schmitt, H. Müller, and K. Kleinermanns, Chem. Phys. Lett. **218**, 246 (1994); (b) A. Schiefke, C. Deusen, C. Jacoby, M. Gerhards, M. Schmitt, and K. Kleinermanns, J. Chem. Phys. **102**, 9197 (1995); (c) M. Schmitt, H. Müller, U. Henrichs, M. Gerhards, W. Perl, Ch. Deusen, and K. Kleinermanns, *ibid*. **103**, 584 (1995); (d) M. Schmitt, U. Henrichs, H. Müller, and K. Kleinermanns, *ibid*. **103**, 9918 (1995); (e) M. Gerhards, W. Perl, S. Schumm, U. Henrichs, C. Jacoby, and K. Kleinermanns, *ibid*. **104**, 9362 (1996).
[7] M. Schütz, T. Bürgi, and S. Leutwyler, J. Chem. Phys. **98**, 3763 (1993).
[8] R. M. Helm, H.-P. Vogel, and H. J. Neusser, J. Chem. Phys. **108**, 4496 (1998), following paper.
[9] D. Feller and M. W. Feyereisen, J. Comput. Chem. **14**, 1027 (1993).
[10] O. Dopfer, G. Riser, K. Müller-Dethlefs, E. W. Schlag, and S. D. Colson, J. Chem. Phys. **101**, 974 (1994).
[11] Hobza, R. Burcl, V. Špirko, O. Dopfer, K. Müller-Dethlefs, and E. W. Schlag, J. Chem. Phys. **101**, 990 (1994).
[12] T. Ebata, M. Furukawa, T. Suzuki, and M. Ito, J. Opt. Soc. Am. B **7**, 1890 (1990).
[13] R. J. Stanley and A. W. Castleman, Jr., J. Chem. Phys. **94**, 7744 (1991).
[14] R. J. Stanley and A. W. Castleman, Jr., J. Chem. Phys. **98**, 796 (1993).
[15] S. Tanabe, T. Ebata, M. Fujii, and N. Mikami, Chem. Phys. Lett. **215**, 347 (1993).
[16] T. Watanabe, T. Ebata, S. Tanabe, and N. Mikami, J. Chem. Phys. **105**, 408 (1996).
[17] A. Oikawa, H. Abe, N. Mikami, and M. Ito, J. Phys. Chem. **87**, 5083 (1983).
[18] H. Abe, N. Mikami, and M. Ito, J. Phys. Chem. **86**, 1768 (1982).
[19] K. Fuke and K. Kaya, Chem. Phys. Lett. **94**, 97 (1983).
[20] A. Goto, M. Fujii, N. Mikami, and M. Ito, J. Phys. Chem. **90**, 2370 (1986).
[21] A. Sur and P. M. Johnson, J. Chem. Phys. **84**, 1206 (1986).
[22] R. J. Lipert and S. D. Colson, J. Chem. Phys. **89**, 4579 (1988).
[23] R. J. Lipert, G. Bermudez, and S. D. Colson, J. Phys. Chem. **92**, 3801 (1988).
[24] R. J. Lipert and S. D. Colson, J. Phys. Chem. **93**, 135 (1989).
[25] R. J. Lipert and S. D. Colson, J. Phys. Chem. **94**, 2358 (1990).
[26] K. Müller-Dethlefs, M. Sander, and E. W. Schlag, Z. Naturforsch. Teil A **39**, 1089 (1984).
[27] R. J. Lipert and S. D. Colson, J. Chem. Phys. **92**, 3240 (1990).
[28] K. Müller-Dethlefs, M. Sander, and E. W. Schlag, Chem. Phys. Lett. **112**, 291 (1984).
[29] G. Reiser, O. Dopfer, R. Lindner, G. Henri, K. Müller-Dethlefs, E. W. Schlag, and S. D. Colson, Chem. Phys. Lett. **181**, 1 (1991).
[30] O. Dopfer, G. Reiser, R. Lindner, and K. Müller-Dethlefs, Ber. Bunsenges. Phys. Chem. **96**, 1259 (1992).
[31] O. Dopfer and K. Müller-Dethlefs, J. Chem. Phys. **101**, 8508 (1994).
[32] GAUSSIAN 94, Revision B.3, M. J. Frisch, G. W. Trucks, H. B. Schlegel, P. W. M. Gill, B. G. Johnson, M. A. Robb, J. R. Cheeseman, T. Keith, G. A. Petersson, J. A. Montgomery, K. Raghavachari, M. A. Al-Laham, V. G. Zakrzewski, J. V. Ortiz, J. B. Foresman, C. Y. Peng, P. Y. Ayala, W. Chen, M. W. Wong, J. L. Andres, E. S. Replogle, R. Gomperts, R. L. Martin, D. J. Fox, J. S. Binkley, D. J. Defrees, J. Baker, J. P. Stewart, M. Head-Gordon, C. Gonzalez, and J. A. Pople, Gaussian, Inc., Pittsburgh, PA, 1995.
[33] Otto Dopfer, Dissertation Technische Universität München 1995.
[34] J. D. Lewis, T. B. Malloy, T. H. Chao, and J. Laane, J. Mol. Struct. **12**, 427 (1972).
[35] W. Press, S. Teukolsky, W. Vetterling, and B. Flannery, *Numerical Recipes in FORTRAN*, 2nd ed. (Cambridge University Press, Cambridge, 1994).
[36] H. C. Longuet-Higgins, Mol. Phys. **6**, 445 (1963).